spacing of either $d_{20\bar{2}0}$ or $d_{30\bar{3}0}$. Because of the threefold axis we choose $d_{30\bar{3}0}$ as the most probable one.

Positions associated with one threefold axis and lying within the unit cell are (x,y,z), $(1-y,1+x-y, z+\frac{1}{3})$, $(y-x,1-x,z+\frac{2}{3})$. From equation (1) we find:

$$(1-y_m)-(x_m)=\tfrac{1}{3} \text{ and } (y_m-x_m)-(1-y_m)=\tfrac{1}{3},$$

from which $x_m=0$ and $y_m=\frac{2}{3}$.

The average of 22 atoms is: $x_m=0{\cdot}0899$, $y_m=0{\cdot}6715$ and $z_m=0{\cdot}07611$, whereas the predicted values are: $x_m=0$, $y_m=0{\cdot}6667$ and $z_m=0{\cdot}08333$.

The idealized position $(0,\frac{2}{3},1/12)$ and its equivalents form a rhombohedral sublattice with $a_{rh}=(\frac{1}{3})[1\bar{1}01]=13{\cdot}141$ Å and $\alpha_{rh}=37°30'$. Each molecule is surrounded by ten molecules (see Fig. 3), one at a distance 6·101 Å (bond p), three at a distance 7·811 Å (bond q) and six at a distance 8·449 Å (bond r).

These last six bonds occur in a slice d_{0006}. However, the form {0001} has not been observed and therefore the bonds r will be weak, so we are left with one bond p and three bonds q for each molecule. One bond p and one bond q constitute together a *PBC*, the period of which is equal to the edge of the rhombohedral subcell. The rhombohedron determined by these bonds is $\{\bar{1}011\}$ and not $\{10\bar{1}1\}$ as described by Craven (1964). A slice $d_{\bar{1}011}$ is shown in Fig. 3(*b*).

It may be remarked that the molecular packing can be considered as a distorted diamond or arsenolite structure.

Conclusion

The foregoing examples show that sometimes the observed morphology is not in accordance with the morphology predicted from cell dimensions and space group by a reversed application of the law of Donnay and Harker. In these cases it is possible to locate approximately the centres of molecules.

Further information on the position of these centres can be obtained by applying the *PBC* method. It gives information either about one or two of the coordinates of the centres, or about bond strengths, and it further corroborates the location of the centre.

In this way such structural features as complete or partial pseudosymmetry are easily revealed. This may be a useful clue in arriving at a trial model of the structure in the early stages of a structure analysis.

References

CRAVEN, B. M. (1964). *Acta Cryst.* **17**, 396.

DONNAY, J. D. H. & HARKER, D. (1937). *Amer. Min.* **22**, 446.

DONNAY, J. D. H. & DONNAY, G. (1961*a*). *C. r. Acad. Sci. Paris*, **252**, 908.

DONNAY, J. D. H. & DONNAY, G. (1961*b*). *Ann. Rep. Geophys. Lab. Carnegie Inst., Washington D.C.*, 1960/1961, 208.

DRENTH, J. & JANSONIUS, J. N. (1966). Private communication.

HARKER, D., KING, M. V., PIGNATARO, E. H., ADELMAN, M. B. & FURNAS JR., T. C. (1957). *Acta Cryst.* **10**, 816.

HARTMAN, P. & PERDOK, W. G. (1955). *Acta Cryst.* **8**, 49.

HARTMAN, P. & PERDOK, W. G. (1956). *Amer. Min.* **41**, 449.

HARTMAN, P. (1963). *Z. Kristallogr.* **119**, 65.

HAZELL, A. C., WIEGERS, G. A. & VOS, A. (1966). *Acta Cryst.* **20**, 186.

KING, M. V. (1965). *Acta Cryst.* **18**, 686.

LINDENBERG, W. (1956). *N. J. Miner. Abhandl.* **89**, 149.

PALM, J. H. (1966). *Acta Cryst.* **21**, 473.

WIEGERS, G. A. (1963). Thesis, Groningen, p.25.

Acta Cryst. (1968). A**24**, 364

Diffraction of X-rays by the Faulted Cylindrical Lattice of Chrysotile I. Numerical Computation of Diffraction Profiles

BY K. TOMAN*† AND A. J. FRUEH, JR.

Crystallographic Laboratory, McGill University, Montreal, P.Q., Canada

(*Received* 30 *June* 1967 *and in revised form* 19 *September* 1967)

The current theory of the diffraction of X-rays by a cylindrical lattice is supplemented, and the influence of some misfit boundaries discussed. The numerical computation of diffraction profiles of some reflexions was carried out, and the influence of the curvature, wall thickness, incompleteness and the presence of several types of misfit boundaries determined.

Introduction

The theoretical aspects of the diffraction of X-rays by a cylindrical lattice of chrysotile were studied very thoroughly by Jagodzinski & Kunze (1954*a*,*b*,*c*) and by Whittaker (1955*a*,*c*), who derived formulae for the diffracted intensity by the ideal complete cylindrical lattice, and discussed the influence of azimuthal misfits. Kunze (1956*a*,*b*) derived formulae for the diffracted intensity by the ideal incomplete cylindrical lattice.

The object of this paper is to give a more complete analysis of the form of diffraction profiles, based on

* Nicolet Fellow.

† Permanent Address: Institute of Macromolecular Chemistry, Czechoslovak Academy of Sciences, Prague, Czechoslovakia.

numerical computations carried out with the IBM 7044 system in the Computing Centre of McGill University. For this purpose the expressions for the diffracted intensity, both for complete and incomplete cylinders, were derived by the same method [similar to the one used by Waser (1955)], so that the formulae for both cases are easily comparable. In addition to this, the influence of some defects of the cylindrical lattice on the diffraction intensity not considered in the above-noted papers was studied.

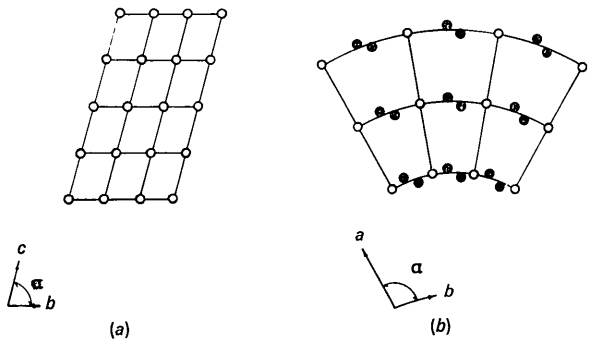

Fig. 1. (*a*) The atomic net of a cylindrical lattice. (*b*) The projection of a cylindrical lattice consisting of 9 atomic nets.

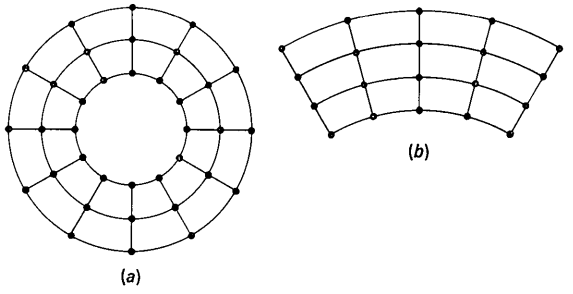

Fig. 2. The complete (*a*), and incomplete (*b*) cylindrical lattice.

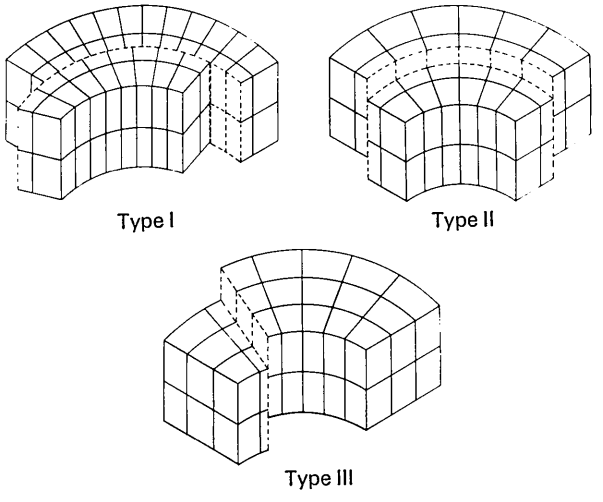

Fig. 3. The cylindrical lattice with (*a*) cylindrical azimuthal boundary, (*b*) cylindrical axial boundary, (*c*) planar axial boundary.

Defects of coherence of the cylindrical lattice

This paper is confined to the anorthic cylindrical lattice (Whittaker, 1955*b*) consisting of coaxial cylindrical nets each of which is occupied by only one sort of atom [Fig. 1(*a*)]. If these coaxial cylindrical nets, having different diameters but the same number of **b** translations subtended by a unit azimuthal angle, are stacked in such a way that they compose a quasi-periodic assembly, we get a three-dimensional lattice which we call an *ideal cylindrical crystal.* Fig. 1(*b*) shows a projection of such a lattice consisting of 9 coaxial nets. We call such a lattice ideal because it can be transformed by an appropriate elastic deformation into the conventional ideal three-dimensional translation lattice. The ideal cylindrical crystal can be complete if circular cylindrical nets are closed [Fig. 2(*a*)] or incomplete [Fig. 2(*b*)].

The regularity of the ideal cylindrical lattice can be disturbed in such a way that the cylindrical crystal consists of mosaic blocks separated by some type of misfit boundary. In this paper we shall consider the following types of misfit boundaries.

Type I. *Cylindrical azimuthal boundary.* This boundary has the form of a coaxial cylindrical surface and separates two azimuthally displaced mosaic blocks. The number of translations in the azimuthal direction *b* per unit angle can be different in both blocks, but there is no relative displacement between the blocks along the direction of the axis of the cylinder [Fig. 3(*a*)].

Type II. *Cylindrical axial boundary.* The boundary is a coaxial cylindrical surface separating two mosaic blocks axially shifted. The number of translations in both blocks per unit angle is the same and both blocks have no relative azimuthal displacement [Fig. 3(*b*)].

Type III. *Planar axial boundary.* The boundary is formed by a plane containing the cylinder axis and a radius *a*. The blocks are axially shifted only [Fig. 3(*c*)].

Type IV. *Planar incoherent boundary.* The boundary is formed by a plane as in type III. The plane separates two mosaic blocks that are axially radially and angularly displaced, so that the lattices of both blocks are completely independent.

The cylindrical axial and the cylindrical azimuthal boundary (types I and II) can be combined in such a way that the resulting cylindrical boundary has an axial as well as an azimuthal component.

The intensity of radiation diffracted by an ideal cylindrical lattice

Imagine the cylindrical crystal as an assembly of complete or incomplete coaxial cylindrical nets, and every

net as an assembly of parallel circular (complete or incomplete) chains. First, we shall derive the amplitude of radiation diffracted by a chain having the form of a circular arc lying in a plane perpendicular to the axis of the cylinder. It is convenient to use a cylindrical coordinate system (ϱ, z, φ in direct space and ξ, ζ, ω in reciprocal space). A chain in the jth coaxial cylindrical net contains N atoms with atomic scattering factor f_j; its radius is ϱ_j and the repeat distance of the atom along the chain is b_j. The νth atom of the μth chain in this jth net has the coordinates $\varrho_j, z_{j\mu}, \varphi_{j\mu\nu}$.

The amplitude $A_{j\mu}$ is thus:

$$A_{j\mu}(\xi,\omega,\zeta)= f_j \exp(2\pi i\zeta z_{j\mu}) \sum_{\nu=0}^{N=1} \exp[2\pi i\xi\varrho_j \cos(\omega-\varphi_{j\mu\nu})] .$$

Using:

$$\exp(2\pi i x\cos\alpha)= \sum_{k=-\infty}^{\infty} i^k J_k(2\pi x)\exp(ik\alpha)$$

and

$$\sum_{\nu=0}^{N-1} \exp(i\nu x)=\exp[ix(N-1)/2]\frac{\sin Nx/2}{\sin x/2}$$

and expressing:

$$\varphi_{j\mu\nu}=\varphi_{j\mu}+\nu b_j/\varrho_j=\varphi_{j\mu}+2\pi\nu/\mathcal{N} ,$$

where $\varphi_{j\mu}$ is the azimuthal coordinate of the origin of the μth chain on the jth cylindrical net and $\mathcal{N}=2\pi\varrho_j/b_j$ we get:

$$A_{j\mu}(\xi,\omega,\zeta)=f_j \exp(2\pi i\zeta z_{j\mu}) \sum_{k=-\infty}^{\infty} {}_1W_k J_k(2\pi\xi\varrho_j) \exp[ik(\omega-\varphi_{j\mu}+\pi(N-1)/\mathcal{N}+\pi/2)] . \quad (1)$$

Here $J_k(2\pi\xi\varrho_j)$ is the Bessel function of the kth order and the weight factor, W_k is given as:

$${}_1W_k=\frac{\sin\pi kN/\mathcal{N}}{\sin\pi k/\mathcal{N}} . \quad (2a)$$

For the special case of a circular chain we have $\mathcal{N}=N$, therefore:

$${}_2W_k=\begin{cases}\mathcal{N} \text{ if } k=\lambda\mathcal{N}, \text{ where} \\ \qquad \lambda \text{ is an integer} \\ 0 \quad \text{for the remaining } k .\end{cases} \quad (2b)$$

Another interesting special case occurs if we suppose the electron density distribution along the arc is constant and the integral number of electrons is unchanged. Then the weight factor ${}_3W_k$ for an arc with central angle φ becomes:

$${}_3W_k=2\pi\varrho_j\sigma \sin k\varphi/k\varphi , \quad (2c)$$

where σ is the number of electrons on unit length. For the complete circle we get:

$${}_4W_k=2\pi\varrho_j\sigma \quad \text{if} \quad k=0$$
$$W_k=0 \quad \text{if} \quad k\neq 0 .$$

The distributions ${}_1W_k, {}_2W_k, {}_3W_k, {}_4W_k$ are shown in Fig. 4.

The amplitude of radiation diffracted by the jth cylindrical net is given by $A_j=\sum_{\mu=0}^{M-1} A_{j\mu}$, where M is the number of chains comprising the jth net.

Because

$$\varphi_{j\mu}=\varphi_j+\mu c(\cos\alpha)/\varrho$$

and

$$z_{j\mu}=z_j+\mu c \sin\alpha ,$$

where φ_j and z_j are the azimuthal and axial coordinates of the origin of the jth net, we have:

$$A_j(\xi,\omega,\zeta)=\exp[2\pi i\zeta c(\sin\alpha)(M-1)/2] \sum_{k=-\infty}^{\infty} \Phi_{jk} \exp[ik(\omega+\pi(N-1)/\mathcal{N}+\pi/2)] ,$$

where:

$$\Phi=f_j \exp(2\pi\zeta z_j W_k)\frac{\sin\pi Mc(\zeta\sin\alpha-(k/2\pi\varrho_j)\cos\alpha)}{\sin\pi c(\zeta\sin\alpha-(k/2\pi\varrho_j)\cos\alpha)} \times J_k(2\pi\xi\varrho_j)\exp\{-ik[\varphi_j-(M-1)(c\cos\alpha)/2\varrho_j]\} .$$

The amplitude of the radiation diffracted by the assembly of coaxial nets is:

$$A=\sum_j A_j=\exp[2\pi i\zeta(c\sin\alpha)(M-1)/2] \sum_j \sum_{k=-\infty}^{\infty} \Phi_{jk} \exp\{ik[\omega+\pi(N-1)/\mathcal{N}+\pi/2]\} . \quad (3)$$

The intensity of the diffracted radiation is:

$$I=|A|^2=\sum_j\sum_{j'}\sum_k\sum_{k'} \Phi_{jk}\Phi^*_{jk} \exp[i\omega(k-k')] \exp[i\pi(k-k')(N-1+\mathcal{N}/2)/\mathcal{N}] .$$

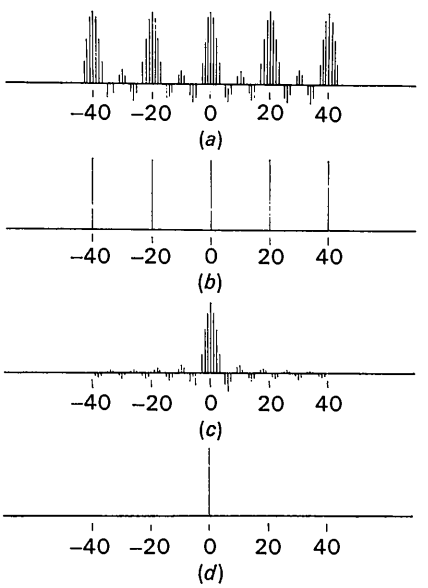

Fig. 4. The distribution of the weight coefficient W_k for: (*a*) the incomplete cylindrical lattice, $\mathcal{N}=20$, $N=5$; (*b*) the complete cylindrical lattice, $\mathcal{N}=20$; (*c*) the incomplete cylindrical lattice with constant electron density along the arcs of $\pi/2$ azimuthal extent; (*d*) the complete cylindrical lattice with constant electron density along the arcs.

The intensity diffracted by a single cylindrical crystal cannot be measured, because samples of the size used in X-ray experiments consist of millions of parallel crystals differently oriented about the cylindrical axis. The measured intensity is thus:

$$I_{\text{meas}}=\langle I\rangle_\omega$$

and as:

$$\langle\exp[i\omega(k-k')]\rangle_\omega=\begin{cases}1 & \text{if } k=k'\\ 0 & \text{if } k\neq k'\end{cases}$$

we have:

$$I_{\text{meas}}=\sum_{k=-\infty}^{\infty}\Big|\sum_j \Phi_{jk}\Big|^2 . \tag{4}$$

Intensity diffracted by a mosaic cylindrical crystal

Type I. *Cylindrical azimuthal boundary*

Consider an assembly of cylindrical crystals, each of which contains the same number of azimuthal boundaries dividing it into mosaic blocks of the same size. The crystals of our assembly differ only in the magnitude of azimuthal displacements corresponding to the individual boundaries. Let us further assume that the sample consists of such a number of parallel cylindrical crystals that every variant occurs with such a variety of orientations that it is possible to average independently over ω. In the ideal cylindrical crystal φ_j, the azimuthal coordinate of the origin of the jth cylindrical net was determined by the inner structure of the lattice. In the pth mosaic crystal of the assembly the azimuthal coordinate of the origin of the jth cylindrical net is given by the expression $\varphi_j+\Delta\varphi_{jp}$ where $\Delta\varphi_{jp}$ has the same numerical value for all cylindrical nets belonging to the same mosaic block of the pth mosaic crystal.

The intensity diffracted by the pth mosaic crystal is thus:

$$I_p=|A_p|^2=\sum_{jj'}\sum_{kk'}\Phi_{jk}\Phi^*_{j'k'}\,\frac{\exp[i\omega(k-k')\exp[i\pi(k-k')(\mathcal{N}-1+\mathcal{N}/2)/\mathcal{N}]}{\exp[i(k\Delta\varphi_{jp}-k'\Delta\varphi_{j\,p})]}.$$

The mean intensity gained by averaging over ω and p is:

$$I=\langle I_p\rangle_{\omega p}=\sum_k\sum_{jj'}\Phi_{jk}\Phi^*_{j'k}\langle\exp[-ik(\Delta\varphi_{jp}-\Delta\varphi_{j'p})]\rangle_p .$$

The mean value of $\langle\exp[-ik(\varphi_{jp}-\varphi_{j'p})]\rangle_p$ depends on the distribution of $\Delta\varphi_{jp}-\Delta\varphi_{j'p}$ in the assembly. Let us suppose, for simplicity, that $\Delta\varphi_{jp}-\Delta\varphi_{j'p}$ can, with the same probability, assume any value inside the interval $-\alpha_{jj'}, +\alpha_{jj'}$, but that outside this interval it has zero probability. The width of this interval depends on indices j and j' of the cylindrical nets whose contribution we are considering. For example, if indices j and j' refer to two different cylindrical nets of the same mosaic block of the pth mosaic crystal, then $\Delta\varphi_{jp}-\Delta\varphi_{j'p}=0$ for any value of p, and $\alpha_{jj'}=0$. If j and j' refer to two different blocks of the mosaic crystal, the corresponding width of the interval $2\alpha_{jj'}\neq 0$ and cannot be further discussed unless additional assumptions about the statistics of the mosaic structure of our assembly are made. Let us take as the simplest assumption that the azimuthal rotations of the individual mosaic blocks are completely independent. Then $\alpha_{jj'}A$ is a constant independent of j and j' unless j and j' refer to the cylindrical nets of the same mosaic block.

With these assumptions, $I=\sum_k\sum_{jj'}\Phi_{jk}\Phi^*_{j'k}(\sin\alpha_{jj'}k)/\alpha_{jj'}k$. It remains to specify $\alpha_{jj'}$. Let us suppose that the rotations correspond to a few translations b_j, so that $\alpha_{jj'}\sim nb_j/\varrho_j$, where n is a small integer. Consider the simpler case of the complete cylindrical crystal where $k=\lambda\mathcal{N}_j$, with λ an integer and $\mathcal{N}_j$ the number of unit-cell translations **b** along with circumference of the jth cylindrical net. Then $k\alpha_{jj'}\sim\lambda\mathcal{N}_jb_j/\varrho_j=2\pi\lambda n$, if j and j' refer to the different mosaic blocks, and the function $(\sin k\alpha_{jj'})/k\alpha_{jj'}$ has the following values:

	$k=0$	$k\geq\mathcal{N}$
j and j' refer to the same block	1	1
j and j' refer to two different blocks	1	small number .

With the use of these results the average intensity is:

$$I=\Big|\sum_j^{\text{whole}}\Phi_{j0}\Big|^2+\sum_{\lambda=-\infty}^{\infty}{}'\Big[\Big|\sum_j^1\Phi_{j\lambda}\Big|^2+\Big|\sum_j^2\Phi_{j\lambda}\Big|^2+\ldots+\Big|\sum_j^s\Phi_{j\lambda}\Big|^2\Big], \tag{5a}$$

where $\sum_j^{\text{whole}}$ means summation over all cylindrical nets in the whole mosaic crystal, and $\sum_j^1, \sum_j^2, \ldots, \sum_j^s$ summations over cylindrical nets in the 1st, 2nd and sth mosaic blocks respectively. The summation $\sum_{\lambda=-\infty}^{\infty}{}'$ does not contain the term with $\lambda=0$. The interpretation of the expression (5*a*) is then as follows: the terms containing Bessel functions of zero order do not contain any information about the azimuthal distribution of the electron density [this can be seen from equations (2*d*) and (3)]. For these terms the entire mosaic crystal diffracts as one coherent domain (*i.e.* the sum of the amplitudes is squared). For the terms containing high order Bessel functions the individual blocks of mosaic diffract as coherent domains.

In the case of an incomplete cylindrical crystal, k can be any integer, so that for $0<k<\mathcal{N}$, $(\sin k\alpha_{jj'})/k\alpha_{jj'}$ has intermediate values. However, as can be seen in Fig. 4(*a*), the contributions are significant only in the

neighbourhood of $k=\lambda\mathscr{N}$, unless the angular range of the incomplete cylindrical crystal is too small. With this restriction the approximate formula can be written:

$$I=\sum_{k}^{*}\Big|\sum_{j}^{\text{whole}}\Phi_{jk}\Big|^2+\sum_{k}'\Big[\Big|\sum_{j}^{1}\Phi_{jk}\Big|^2+\Big|\sum_{j}^{2}\Phi_{jk}\Big|^2+\ldots+\Big|\sum_{j}^{s}\Phi_{jk}\Big|^2\Big]. \quad (5b)$$

Here $\sum_{k}^{*}$ refers to k's corresponding to the maximum about $k=0$ in Fig. 4, $\sum_{k}'$ refers to the remaining k's.

The first term in formula (5*b*) corresponds approximately to the contribution from the assembly of circular arcs having a constant electron density [compare Fig. 4(*a*) and 4(*c*)] and the same central angle φ as the chains in the incomplete cylindrical crystal.

The individual blocks separated by azimuthal boundaries do not necessarily have the same number of translations for a unit of azimuthal angle. The sth block can have $\mathscr{N}_s$ translations with $\mathscr{N}_s$ increasing proportionally with ϱ_s, the mean radius of the sth block. This enables us to reduce substantially the strain energy in our models, which, for an ideal cylindrical crystal even with a wall thickness of a few translations, is intolerable. This point was stressed earlier in the papers of Whittaker and of Kunze.

Type II. *Cylindrical axial boundary*

Let us suppose a similar assembly of mosaic crystals as was considered in the previous case. The only difference is that the shifts of mosaic blocks are now axial. In the ideal cylindrical crystal the axial coordinate z_j of the origin of the jth cylindrical net was determined only by the inner structure of the lattice. Here it is given by $z_j+\Delta z_{jp}$ where z_j is determined by the structure of the lattice and Δz_{jp} is the axial shift of the jth cylinder in the pth mosaic crystal due to the mosaic disorder. After averaging over ω and p the expression for diffracted intensity is:

$$I=\sum_{k}\sum_{jj'}\Phi_{jk}\Phi_{j'k}^{*}\langle\exp\left[2\pi i\zeta(\Delta z_{jp}-\Delta z_{j'p})\right]\rangle_p .$$

If the same assumptions are made about the distribution of $\Delta z_{jp}-\Delta z_{j'p}$ in this assembly as in the previous case, we get:

$$I=\sum_{k}\sum_{jj'}\Phi_{jk}\Phi_{j'k}^{*}(\sin\zeta\alpha_{jj'})/\zeta\alpha_{jj'} .$$

Assuming the range of axial shifts $2\alpha_{jj'}\sim nc$ for j and j' belonging to different mosaic blocks, and $2\alpha_{jj'}=0$ for j and j' belonging to the same mosaic block, we have for $(\sin\zeta\alpha_{jj'})/\alpha_{jj'}$

	$\zeta=0$	$\zeta\geq 1/c$
j and j' refer to the same block	1	1
j and j' refer to different blocks	1	small .

The first column applies to the equator of the diffraction diagram, the second to the first and higher layer lines.

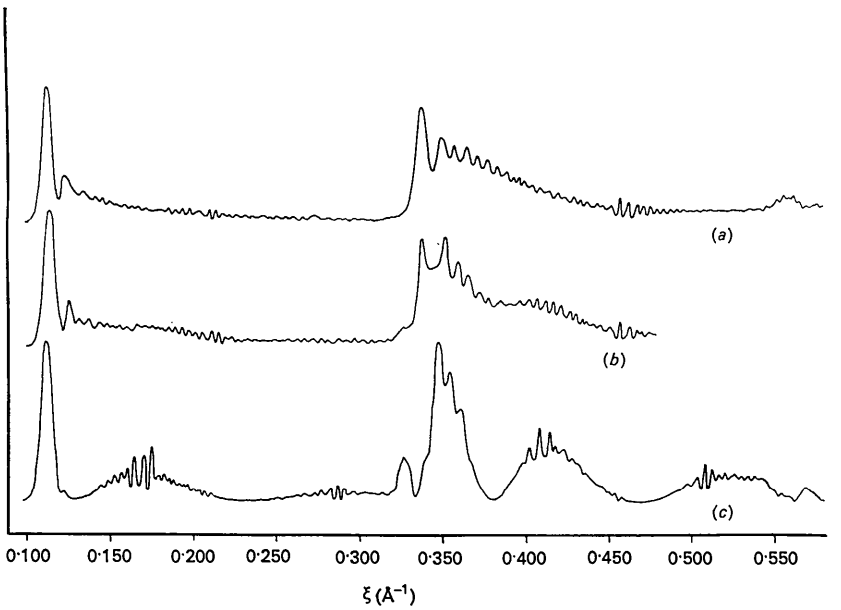

Fig. 5. The distribution of the diffracted intensity on the first layer line diffracted by a model of a complete cylindrical crystal consisting of 10 silica–brucite double layers separated by: (*a*) 9 cylindrical azimuthal boundaries; (*b*) 8 cylindrical azimuthal boundaries similar to the previous model except that the boundary with the largest radius has been omitted; (*c*) 4 cylindrical boundaries equally distributed.

The diffracted intensity is thus:

$$I=\sum_{k=-\infty}^{\infty}\Big|\sum_{j}^{\text{whole}}\Phi_{jk}\Big|^2 \quad \text{if} \quad \zeta=0 \tag{5c}$$

$$I=\sum_{k=-\infty}^{\infty}\Big[\Big|\sum_{j}^{1}\Phi_{jk}\Big|^2+\Big|\sum_{j}^{2}\Phi_{jk}\Big|^2+\ldots+\Big|\sum_{j}^{s}\Phi_{jk}\Big|^2\Big].$$

It can be seen from these equations that for the equatorial diffraction the whole mosaic crystal is a coherent domain, because the equator contains information about the projection of the electron density perpendicular to the equatorial plane only. On the other hand, the diffraction on the upper layer lines is also affected by the z coordinates so that only individual mosaic blocks must be considered as coherent domains.

Type I *and type* II. *Cylindrical azimuthal and cylindrical axial boundaries*

The formula for the diffracted intensity for mosaic crystals containing both axial and azimuthal boundaries is derived in a manner similar to the formula for the individual displacement and is as follows:

$$\text{for } \zeta=0;\ I=\sum_{k}^{*}\Big|\sum_{j}^{\text{whole}}\Phi_{jk}\Big|^2 + \sum_{k}\Big[\Big|\sum_{j}^{1az}\Phi_{jk}\Big|^2+\Big|\sum_{j}^{2az}\Phi_{jk}\Big|^2+\ldots+\Big|\sum_{j}^{qaz}\Phi_{jk}\Big|^2\Big] \tag{5d}$$

$$\text{for } \zeta\geq 1/c,\ I=\sum_{k}^{*}\Big[\Big|\sum_{j}^{1ax}\Phi_{jk}\Big|^2+\sum_{j}^{2ax}\Phi_{jk}\Big|^2+\ldots +\Big|\sum_{j}^{Sax}\Phi_{jk}\Big|^2\Big]+\sum_{k}'\Big[\Big|\sum_{j}^{1}\Phi_{jk}\Big|^2 +\Big|\sum_{j}^{2}\Phi_{jk}\Big|^2+\ldots+\Big|\sum_{j}^{S}\Phi_{jk}\Big|^2\Big].$$

Here the symbols related to the sums over k have the same meaning as previously; $\overset{1az}{\Sigma}, \overset{2az}{\Sigma}, \overset{qaz}{\Sigma}$ denote summations where only the azimuthal mosaic boundaries are considered as limiting the mosaic blocks; $\overset{1ax}{\Sigma}, \overset{2ax}{\Sigma}, \overset{sax}{\Sigma}$ are summations considering only the axial boundaries and neglecting the azimuthal ones; $\overset{1}{\Sigma}, \overset{2}{\Sigma}, \overset{s}{\Sigma}$ are summations where there is no difference made between axial and azimuthal boundary.

Type III. *Planar axial boundary*

Let us consider an assembly of parallel cylindrical mosaic crystals, where the mosaic block boundaries are of the planar axial type. Every mosaic crystal has N translations in the direction of the b axis, divided in s mosaic blocks in such a way that the first block has N_1, the second N_2, and the last N_s translations. Individual mosaic crystals again differ only in the magnitude of axial shifts of mosaic blocks; otherwise they are identical.

In the previous case atoms of the three-dimensional cylindrical lattice grouped into a number of two-dimensional cylindrical nets (j=constant) were considered. Shifts of Δz_j caused by the presence of cylindrical axial mosaic boundaries were associated with them.

In this case atoms are grouped in two-dimensional planar nets, (ν=constant) shifted by $\Delta z_{\nu p}$ owing to the presence of axial planar boundaries.

The intensity of radiation diffracted by the pth mosaic crystal is thus:

$$I_p=|A_p|^2=\Big|\sum_{\nu=0}^{N-1}\sum_{\mu=0}^{M-1}\sum_{j}^{\text{whole}} f_j \exp\left[2\pi i\zeta(z_{j\mu}+\Delta z_{\mu p})\right]\exp\left[2\pi i\varrho_j\cos(\omega-\varphi_{j\mu\nu})\right]\Big|^2.$$

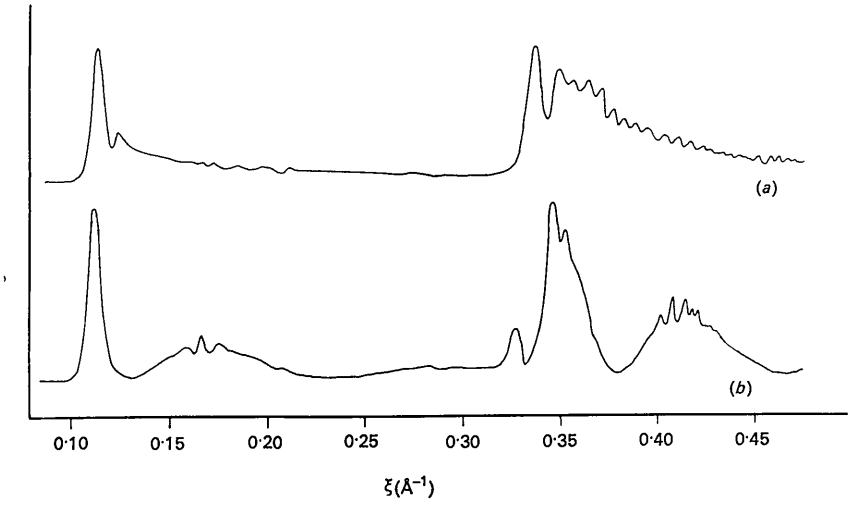

Fig. 6. The distribution of the diffracted intensity on the first layer line diffracted by a model of an incomplete cylindrical crystal with azimuthal extension of π. Crystal consists of 10 silica–brucite double layers separated by (*a*) 9 equally spaced cylindrical azimuthal boundaries, (*b*) 4 equally spaced cylindrical azimuthal boundaries.

Inserting for $z_{j\mu}$ and $\varphi_{j\mu\nu}$ and summing over j and μ

$$I_p=|\sum_{k=-\infty}^{\infty}\sum_{\nu=0}^{N=1}\exp\left[ik(\omega-2\nu/\mathcal{N})]\psi_k i^k\exp 2\pi i\zeta\Delta z_{\nu p}\right]|^2,$$

where

$$\psi_k=\sum_{j}^{\text{whole}}\frac{\sin\pi Mc(\zeta\sin\alpha-(k/2\pi\varrho_j)\cos\alpha)}{\sin\pi c(\zeta\sin\alpha-(k/2\pi\varrho_j)\cos\alpha)}\times\exp\left[2\pi i\zeta z_j\right]J_k(2\pi\xi\varrho_j)\exp\left\{-ik[\varphi_j+(M+1)\times(\cos\alpha)/2\varrho_j]\right\}.$$

Averaging over ω and p we get the mean intensity:

$$I=\sum_{k=-\infty}^{\infty}\sum_{\nu=0}^{N-1}\sum_{\nu'=0}^{N-1}|\psi_k|^2\exp\left[2\pi ik(\nu-\nu')/\mathcal{N}\right]\times\langle\exp\left[2\pi i\zeta(\Delta z_{\nu p}-\Delta z_{\nu' p})\right]\rangle_p.$$

Assuming that the distribution of $\Delta z_{\nu p}-\Delta z_{\nu' p}$ has the same properties as the distribution of $\Delta z_{j p}-\Delta z_{j' p}$ we have:

$$\zeta=0,\ I=\sum_{k=-\infty}^{\infty}\left|\sum_{\nu=0}^{\text{whole}}\psi_k\exp\left(2\pi ik\nu/\mathcal{N}\right)\right|^2=\sum_{k=-\infty}^{\infty}|\psi_k|^2\frac{\sin^2\pi kN/\mathcal{N}}{\sin^2\pi k/\mathcal{N}}$$

$$\zeta\geq 0,\ I=\sum_{k=-\infty}^{\infty}|\psi_k|^2\left[\frac{\sin^2\pi kN_1/\mathcal{N}}{\sin^2\pi k/\mathcal{N}}+\frac{\sin^2\pi kN_2/\mathcal{N}}{\sin^2\pi k/\mathcal{N}}+\ldots+\frac{\sin^2\pi kN_s/\mathcal{N}}{\sin^2\pi k/\mathcal{N}}\right].\quad(5e)$$

As in the case of cylindrical axial boundaries, for the equatorial reflexions the whole mosaic crystal is a coherent domain. For layer lines individual mosaic blocks are independent domains.

Type IV. *Planar incoherent boundaries*

If we assume that the mosaic blocks separated by planar incoherent boundaries are completely independent, then the diffracted intensity is the sum of the intensities diffracted by individual mosaic blocks (incomplete cylindrical lattices).

The programs for the computation of expressions (5*a*), (5*b*), and (5*d*) were written in the Fortran 4 language for the IBM 7044 system. The following limitations were introduced because of practical considerations:

(i) In summations over k, only terms with $J_k(2\pi\xi\varrho_j)\geq e^{-10}$ are included.

(ii) In case of incomplete cylinders, only contributions with $W_k^2\geq W_0^2/100$ are included.

Even with this limitation the computing was very time-consuming, so that for a model with a mean radius

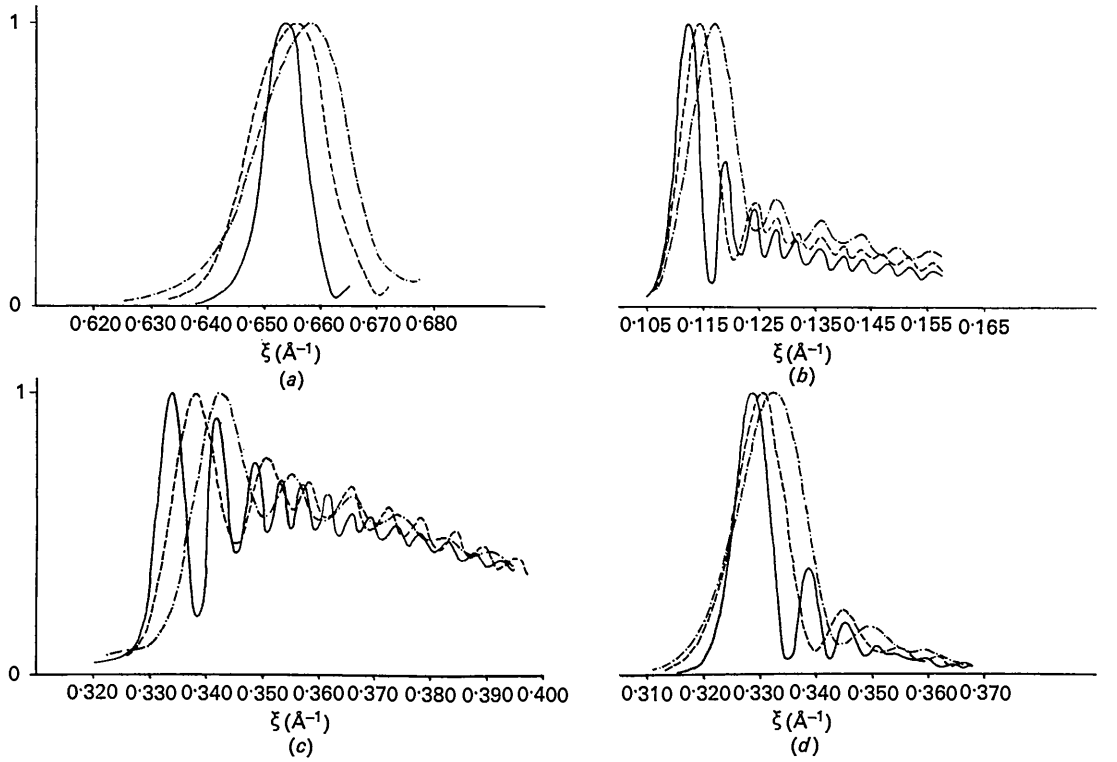

Fig. 7. Some diffraction profiles computed for the model of the complete cylindrical lattice consisting of 10 silica–brucite double layers separated by 9 cylindrical azimuthal boundaries. Mean radius 85 Å shown by dot-dashed line, 135 Å by dashed line, 235 Å by solid line. (*a*) 060; (*b*) 011; (*c*) 031; (*d*) 033.

135 Å and a wall thickness of 5 translations the computation of one point of the intensity curve 011 took 5 sec for a complete cylindrical crystal, and 150 sec for an incomplete one (arc of 45°). For larger mean radii the computing time was longer.

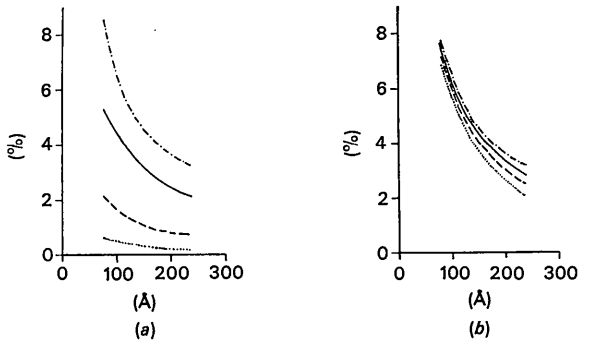

Fig. 8. The per cent relative shift *versus* the mean radius of (*a*) the reflexions 011, 031, 033 and 060 (top to bottom) for the complete cylindrical lattice of the same type as in Fig. 7, (*b*) the 011 reflexion for the cylindrical lattice of different completeness. From top to bottom, complete cylinder, $\frac{1}{2}$ cylinder, $\frac{1}{4}$ cylinder, $\frac{1}{8}$ cylinder. The number of double layers and imperfections as in Fig. 7.

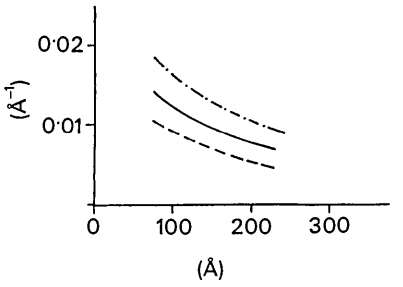

Fig. 9. The dependence of the half-height width of the reflexions 060 (dot-dashed line), 033 (solid line) and 011 (dashed line) on the mean radius of the cylindrical lattice. The number of double layers and imperfections as in Fig. 7.

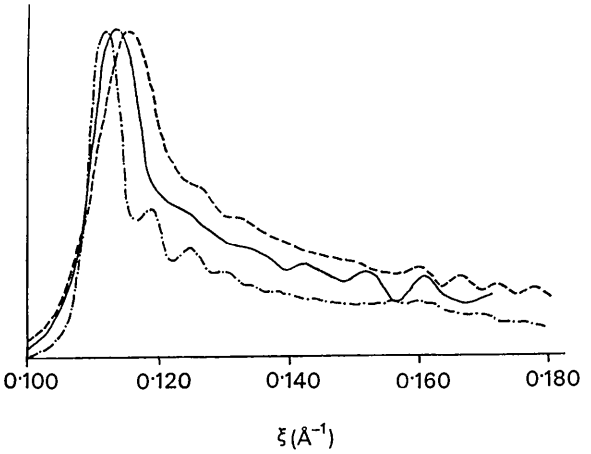

Fig. 10. The profile of the 011 reflexion computed for an incomplete cylindrical lattice with extension $\pi/4$ ($\frac{1}{8}$ of a cylinder) and mean radius 85 Å, dashed line; 135 Å, solid line; and 235 Å, dot-dashed line. The number of double layers and imperfections as for Fig. 7.

The reflexions of X-rays diffracted by the chrysotile lattice can be divided into two groups. One contains reflexions where the intensity is mostly determined by the contributions of the zero-order Bessel functions. These reflexions provide no information about the azimuthal variations of the electron density, as these reflexions are observed even when diffracted by a cylindrical lattice where the electron density does not depend on the azimuth [compare expression (2*d*)]. Their reciprocal coordinates ξ,ζ correspond to the reflexions *h*0*l* of the limiting crystal (the crystal obtained by allowing the radius ϱ of an incomplete cylindrical crystal to approach infinity while preserving its axial orientation). The other group contains reflexions carrying information about the azimuthal distribution of the electron density and about the curvature of the lattice, because the dominant contributors are the terms with higher-order Bessel functions. Their reciprocal coordinates correspond to the reflexions 0*kl* of a limiting crystal. As the behaviour of both groups of reflexion is different when the geometry of the cylindrical crystal is changed, we treat them separately.

Reflexions h0l

The intensity of *h*0*l* reflexions is determined mainly by the zero-order Bessel functions. As already shown by Whittaker (1955*a*), their width is inversely proportional to the wall thickness in almost exactly the same way as it is for the normal linear crystal. By the numerical computation of the profile of the reflexions 200 and 202 of the cylindrical lattice of chrysotile, we found that neither the width nor the position of these reflexions depends on the radius of the cylindrical crystal. The computation was performed for mean radii 85, 135 and 235 Å. It is therefore possible to use reflexions *h*00 for the determination of the overall wall thickness of the cylindrical crystal, and reflexions *h*0*l* for the determination of the radial dimension of a mosaic block separated by cylindrical axial boundaries.

Reflexions 0kl

The form of the reflexions 0*kl* is essentially dependent on the number of azimuthal cylindrical boundaries. This question was already dealt with by Whittaker (1957), who assumed that the chrysotile lattice, consisting of cylindrical double layers (silicate layer and brucite layer), contains the maximum number of azimuthal boundaries; this means that every double layer is separated from the neighbouring one by a cylindrical azimuthal boundary. Every double layer is thus independent and its number of translations *b* on the unit of azimuthal angle increases with increasing mean radius of a mosaic block. This hypothesis is very plausible and leads to the lowest stress in the cylindrical lattice. The diffraction profiles calculated with this assumption do not greatly differ from the experimental ones.

To get a better insight into this question and to have a better basis for the interpretation of the experimentally determined profiles of $0kl$ reflexions, we performed numerical computations of profiles of reflexions lying on the first layer line of the chrysotile diffraction diagram for models having a lower number of cylindrical azimuthal boundaries than the maximum assumed by Whittaker. Our model of the chrysotile fibre has a wall thickness of 5 unit cells and a mean radius 135 Å. The number of translations b on this unit of azimuthal angle corresponds to the mean radius of every mosaic block divided by 9·25 Å. The positions of atoms and unit cell dimensions correspond to those of clinochrysotile, Whittaker (1956). We computed three cases:

1. The model having 10 blocks separated by 9 cylindrical azimuthal boundaries (Whittaker model) [Fig. 5(*a*)].
2. The model having 9 blocks separated by 8 cylindrical azimuthal boundaries, distributed in such a way that the block with the largest radius contains two double layers. This arrangement has the lowest stress energy of all possible cases of 10 double layers distributed among 9 mosaic blocks [Fig. 5(*b*)].
3. The model having 5 blocks separated by 4 cylindrical azimuthal boundaries. Every mosaic block contains two double layers [Fig. 5(*c*)].

Figs. 6(*a*) and (*b*) are the results of similar computations performed for the incomplete cylindrical crystal with azimuthal extension π. The considerable sensitivity of the form of the profile (especially 031) can be deduced from these computations.

One of the most important characteristics of the cylindrical crystal is its mean radius. Whittaker (1955*b*) pointed out the dependence of the position of reflexions $0kl$ on the mean radius. We have dealt with this question in more detail and performed numerical computations to determine the form of reflexions 060, 011, 031, 033 for the mean radii 85, 135 and 235 Å.

In all our models we used the complete cylindrical crystal with the wall of 5 unit cells devided in 10 mosaic blocks by 9 cylindrical azimuthal boundaries. Results are shown in Fig. 7.

In Fig. 8(*a*) the deviation (the per cent difference between the position of the reflexion due to the cylindrical lattice and the position calculated for the limiting lattice) on the mean radius of the cylindrical lattice is shown for above mentioned models.

In Fig. 8(*b*) the dependence of the deviation on the mean radius is shown for the reflexion 011 for different cases of the incomplete cylindrical lattice (5 unit cells thick, 10 blocks).

Also the widths of the reflexions $0kl$ depend strongly on the mean radius of the cylindrical lattice. In Fig. 9 the dependence of half-height width ($B_{1/2}$) is shown for several $0kl$ reflexions for the same models as used previously.

We can see that $B_{1/2}$ increases with decreasing radius of the lattice. This is caused by increasing strains inside mosaic blocks resulting from the decrease of the radius.

A relatively extensive study was undertaken on the effect of cylinder incompleteness on the form of the reflexion 011. We confined ourselves to the reflexion 011, because the calculation is rather time-consuming and the time needed increases greatly with increasing radial reciprocal coordinate of the reflexion. The computations were performed again for a cylindrical crystal with the wall thickness of 5 a-translations consisting of 10 mosaic blocks separated by 9 cylindrical azimuthal boundaries. The number of b-translations per unit of the azimuthal angle in every mosaic block was again equal to the mean block radius divided by 9·25 Å. In Fig. 10 there are profiles of the 011 reflexion for the

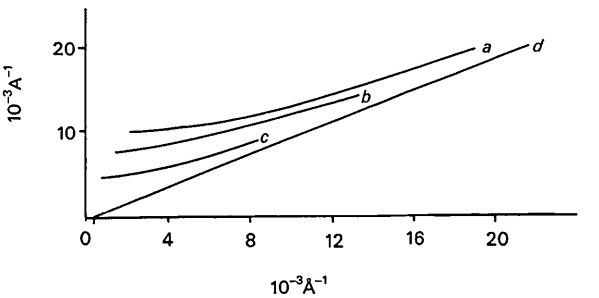

Fig. 11. The half-height width *versus* the reciprocal value of the mean length of arc for incomplete cylindrical lattice of mean radius (*a*) 85 Å; (*b*) 135 Å; (*c*) 235 Å; (*d*) infinite. The numbers of double layers and imperfections are in Fig. 7.

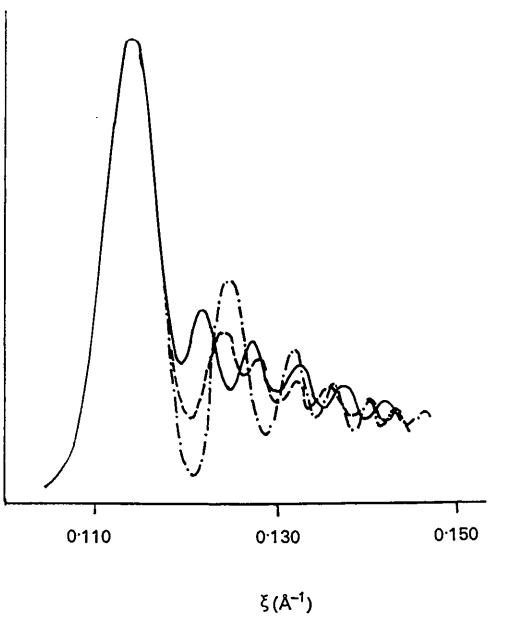

Fig. 12. The influence of the radial wall thickness on the form of the reflexion 011 (mean radius 135 Å). Complete cylindrical lattice with maximum number of cylindrical azimuthal boundaries. Dot-dashed line, 6 double layers; dashed line 10, double layers; solid line, 14 double layers.

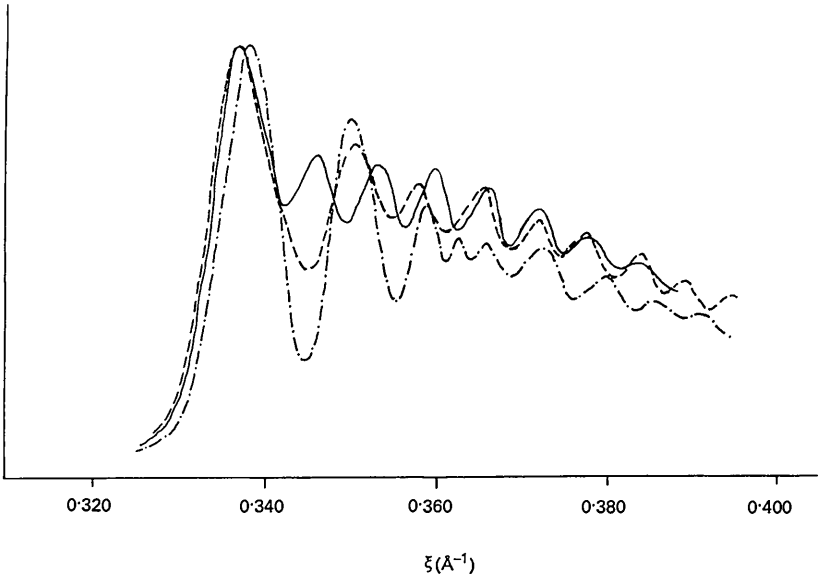

Fig. 13. The influence of the radial wall thickness on the form of reflexion 031. The same models as for Fig. 12.

incomplete crystal of extension $\pi/4$ for mean radii 85, 135 and 235 Å. In Fig. 11 we show the dependence of the half-height width of the 011 reflexion on the reciprocal value of the mean length of arc for the incomplete cylindrical crystals of radii 85, 135 and 235 Å. We can see that with decreasing arc length the curves approach closer to the straight line representing the pure particle-size broadening for a conventional translation lattice.

The influence of the wall thickness of the cylindrical crystal on the diffraction profile 011 and 031 for the same mean radius was also studied (Figs. 12 and 13). The computation was performed for a model of complete cylindrical lattice of chrysotile of wall thicknesses of $3a$, $5a$ and $7a$, split into 6, 10 and 14 mosaic blocks by the cylindrical azimuthal boundaries. We can see that the changes of the wall thickness have only a small effect on the position of the reflexion and on its width. The only major change is in the magnitude of the fluctuations which decrease rapidly with increasing wall thickness.

Conclusions

Within the validity of the foregoing assumptions we can make these conclusions:

1. The wall thickness of the cylindrical lattice can be deduced from the width of zero-order reflexions on the equator ($h00$).
2. The number of mosaic blocks separated by the cylindrical axial boundary can be determined from the ratio of the width of the reflexions on the higher layer lines to those on the equator.
3. The radius of the cylindrical lattice can be determined from the shift of the positions of the reflexions involving high order Bessel functions, especially of 011 and 033.
4. The length of the arc of the incomplete cylindrical lattice (or of the mosaic blocks limited by planar axial or planar incoherent boundaries) can be determined from the width of 011 reflexions.
5. The number of cylindrical azimuthal boundaries can be guessed from the form of the 033 reflexion.

In the next paper we shall apply these results to a number of profile and position measurements of different chrysotile samples.

The authors wish to acknowledge the financial support of the National Research Council of Canada (Operating Grant A-165) and the Nicolet Industries.

References

JAGODZINSKI, H. & KUNZE, G. (1954*a*). *N. Jb. Miner. Mh.* 95.
JAGODZINSKI, H. & KUNZE, G. (1954*b*). *N. Jb. Miner. Mh.* 113.
JAGODZINSKI, H. & KUNZE, G. (1954*c*). *N. Jb. Miner. Mh.* 137.
KUNZE, G. (1956*a*). **9**, 841.
KUNZE, G. (1956*b*). **9**, 847.
WHITTAKER, E. J. W. (1955*a*). *Acta Cryst.* **8**, 261.
WHITTAKER, E. J. W. (1955*b*). *Acta Cryst.* **8**, 571.
WHITTAKER, E. J. W. (1955*c*). *Acta Cryst.* **8**, 726.
WHITTAKER, E. J. W. (1956). *Acta Cryst.* **9**, 855.
WHITTAKER, E. J. W. (1957). *Acta Cryst.* **10**, 149.
WASER, J. (1955). *Acta Cryst.* **8**, 142.